http://ansinet.com/itj

ITJ

ISSN 1812-5638

INFORMATION TECHNOLOGY JOURNAL

ANSInet
Asian Network for Scientific Information
308 Lasani Town, Sargodha Road, Faisalabad - Pakistan

Information Technology Journal 9 (7): 1440-1448, 2010
ISSN 1812-5638

Neural Network Sliding Mode based Current Decoupled Control for Induction Motor Drive

Peng Kang and Zhao Jin
Huazhong University of Science and Technology, China

Abstract: This study deals with the problem of stator currents coupling effect in induction motor drives. In field oriented control, d-axis stator current and q-axis stator current should be regulated independently. However, the stator currents in d-q synchronously rotating reference frame are not naturally decoupled, therefore, a new control scheme for current control is proposed that utilizes Sliding Mode Control (SMC) and Radial Basis Function Neural Network (RBFNN) to achieve the decoupling without considerable chattering. In this control strategy, a RBFNN controller replaces the discontinuous part of the sliding mode controller to eliminate undesired chattering of conventional sliding mode controller. The decoupling method in this study uses two RBFNN sliding mode controllers to regulate d-axis stator current and q-axis stator current, respectively. Finally, simulation results of the proposed scheme have presented perfect performances, such as perfect decoupling, strong robustness and reduced chattering, in comparison with proportional-integral controller and sliding mode controller.

Key words: Current control, decoupling, sliding mode control, radial basis function neural network

INTRODUCTION

In recent years, much research has been done on the field oriented control for high performance of induction motor drives. It is well-known that the current loop is essential to the overall performance of motor drives. Consequently, fast and precise current control methods are research interests at all times.

In general, the coupling action between d-axis stator current and q-axis stator current is not significant in low speed operation and its effect can be ignored. However, in the high speed operation, the effect of this coupling action becomes so obvious that the performance of motors degrades. Several current control methods have been proposed to regulate stator currents. Some typical control strategies include hysteresis control, synchronous PI control, feedforward control and internal mode control (Holtz *et al*., 2002; Harnefors and Nee, 1998; Jung *et al*., 1997). The hysteresis control scheme is easier than other schemes, but the performance of induction motors would deteriorate, due to high harmonic contents of the stator currents. The synchronous PI control scheme can not guarantee the complete decoupling of stator currents dynamics. The feedforward control scheme and internal mode control scheme depend highly on the accuracy of the motor parameters.

Sliding Mode Control (SMC) has many good properties, such as strong robustness, disturbance rejection and easy implementation (Utkin, 1993; Young *et al*., 1999). Sliding mode control is one type of variable-structure control scheme. Normally, two steps, namely the reaching and sliding phases, are necessary in the design of sliding mode controller. Therefore, the sliding mode controller usually consists of an equivalent law and a switching law. The equivalent law is given so that the states can stay on sliding surface. The switching law is used to drive the state trajectory to the sliding manifold. However, usually the switching law is discontinuous part and the frequency of switching in control system is finite high, so undesired chattering exists in control system.

In this study, a new sliding mode control method that can achieve perfect decoupling is proposed. This method combines the merits of sliding mode control and Radial Basis Function Neural Network (RBFNN), in order to eliminate the undesired chattering. In this scheme, we use two RBFNN-sliding mode controller to regulate the d-axis stator current and q-axis stator current respectively. In addition, RBFNN-sliding mode controller is deeply investigated, in which the radial basis function neural network is employed to replace the discontinuous switching law.

FIELD ORIENTED MODEL OF INDUCTION MOTOR

The dynamic model of induction motor in d-q synchronously rotating reference frame is presented as (Bose, 2002; Lasaad *et al*., 2007):

Corresponding Author: Zhao Jin, Huazhong University of Science and Technology, Wuhan, People's Republic of China

$$\begin{aligned}
&\frac{d\omega_r}{dt} = \frac{n_p^2 L_m}{JL_r}(i_{sq}\psi_{rd} - i_{sd}\psi_{rq}) - \frac{n_p}{J}T_l \\
&\frac{d\psi_{rd}}{dt} = -\frac{1}{T_r}\psi_{rd} + (\omega_e - \omega_r)\psi_{rq} + \frac{L_m}{T_r}i_{sd} \\
&\frac{d\psi_{rq}}{dt} = -\frac{1}{T_r}\psi_{rq} - (\omega_e - \omega_r)\psi_{rd} + \frac{L_m}{T_r}i_{sq} \\
&\frac{di_{sd}}{dt} = \frac{L_m}{\sigma L_s L_r T_r}\psi_{rq} + \frac{L_m}{\sigma L_s L_r}\omega_r\psi_{rq} + \omega_e i_{sq} + \frac{u_{sd}}{\sigma L_s} - \frac{R_s L_r^2 + R_r L_m^2}{\sigma L_s L_r^2}i_{sd} \\
&\frac{di_{sq}}{dt} = \frac{L_m}{\sigma L_s L_r T_r}\psi_{rq} - \frac{L_m}{\sigma L_s L_r}\omega_r\psi_{rd} - \omega_e i_{sd} + \frac{u_{sq}}{\sigma L_s} - \frac{R_s L_r^2 + R_r L_m^2}{\sigma L_s L_r^2}i_{sq}
\end{aligned} \tag{1}$$

In above equations, R_s, R_r, L_m, L_s and L_r denote stator resistance, rotor resistance, mutual induction, stator induction and rotor induction, respectively. T_r is rotor time constant; ω_e is motor synchronous angular frequency; ω_r is motor rotor electrical angular frequency; n_p is number of pole pairs; J is rotor moment of inertia; T_l is load torque; u_{sd}, u_{sq} denote d-axis stator current and q-axis stator voltages; i_{sd}, i_{sq} denote d-axis stator current and q-axis stator currents; $\varnothing_{rd}$, $\varnothing_{rq}$ denote d-axis stator current and q-axis rotor flux linkages. Moreover, the total leakage induction coefficient is $\sigma = 1-L_m^2/L_rL_s$.

In order to achieve field oriented control, the d-axis in the synchronously rotating reference frame should be aligned with the rotor flux linkages. Therefore, we have:

$$\begin{aligned}
&\psi_{rd} = \psi_r = \text{const} \\
&\psi_{rq} = 0
\end{aligned} \tag{2}$$

where, $\varnothing_r$ is the amplitude of the rotor flux linkages. Taking Eq. 2 into account, the rotor flux equation and the electromagnetic torque equation can be described as:

$$T_e = n_p(L_m/L_r)\psi_r i_{sq} \tag{3}$$

$$\psi_r = L_m i_{sd}/(1+T_r p) \tag{4}$$

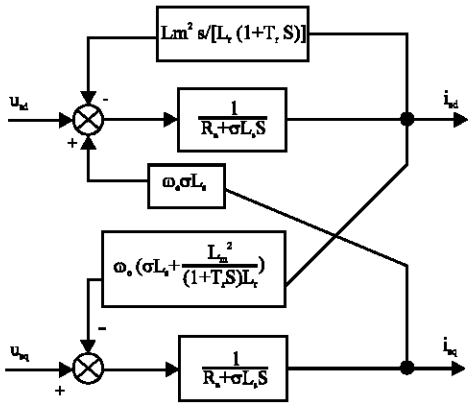

Fig. 1: Block diagram of induction motor

where, p is the derivative operator. And the stator voltage equations can be written as (Ma *et al*., 2005):

$$u_{sd} = (\sigma L_s p + R_s)i_{sd} - \sigma L_s\omega_e i_{sq} + L_m p\psi_r / L_r \tag{5}$$

$$u_{sq} = (\sigma L_s p + R_s)i_{sq} + \sigma L_s\omega_e i_{sd} + L_m\omega_r\psi_r / L_r \tag{6}$$

Based on the above analysis, a block diagram is reasonably presented in Fig. 1. It is obvious that there is coupling action between d-axis stator current and q-axis stator current of induction motor.

DESIGN OF SLIDING MODE CONTROL

The sliding mode control strategy has been widely used as a nonlinear control method. In general, It utilizes a high frequent switch to drive the phase trajectory towards a predetermined sliding surface. Theoretically, the system states can gradually approximate the sliding mode surface, finally they can approach the control objective. In order to design a sliding mode controller, two essential steps should be carefully investigated, namely, the selection of sliding mode surface and the design of control law.

The selection of sliding mode surface is based on desired motion of the system. Considering the simplicity of design, we define sliding mode surfaces $s = [s_1\ s_2]$ as follows (Ma *et al*., 2005):

$$s_1 = i_{sd}^* - i_{sd} \tag{7}$$

$$s_2 = i_{sq}^* - i_{sq} \tag{8}$$

where i_{sd}^* and i_{sq}^* are the reference values of d-axis stator current and q-axis stator current. If the system states are on the sliding mode surfaces, equations $s_1 = 0$ and $s_2 = 0$ can be obtained. Substituting Eq. 7 and 8 into $s_1 = 0$, $s_2 = 0$, we can get as follows:

$$i_{sd}^* = i_{sd} \tag{9}$$

$$i_{sq}^* = i_{sq} \tag{10}$$

The above equations can ensure that the actual values of the stator currents equate the reference values, if the system states stay on the sliding mode surfaces.

In general, there are several forms of the sliding mode control law. One type of control law consists of an equivalent control law u_{equ} and a switch control law u_s. The control law can be described as $u = u_{equ}+u_s$. The

equivalent control law represents the linear part of the control force, which is usually derived from sliding mode surface and the differential of sliding mode surface. So, it highly depends on the parameters of the control model. The switch control law is a discontinuous control law which enforces the system states towards the sliding mode surface. A possible choice of the switching law is $u_s = k_s\text{sign}(s)$, where k is a constant, which is used to represent the maximum of switching control law. And function sign(s) is defined as:

$$\text{sign}(s) = \begin{cases} -1 & \text{if } s<0 \\ 1 & \text{if } s>0 \end{cases} \quad (11)$$

In this study, to define the equivalent control law, we assume that the sliding mode surface is constant, i.e.,

$$s = \dot{s} = 0 \quad (12)$$

From Eq. 5, 6, 9, 10 and 12, we can define the equivalent control laws of d-axis and q-axis stator current controllers, respectively. They can be defined as follows:

$$u_{sd}^{equ} = \frac{RSL_r^2+R_rL_m^2}{L_r^2} i_{sd} - \frac{L_m}{L_rT_r}\psi_r - \sigma L_s\omega_e i_{sq} + \sigma L_s i_{sd}^* \quad (13)$$

$$u_{sq}^{equ} = \frac{RSL_r^2+R_rL_m^2}{L_r^2} i_{sq} + \frac{L_m}{T_r}\omega_r\psi_r + \sigma L_s\omega_e i_{sd} + \sigma L_s i_{sq}^* \quad (14)$$

where, the rotor flux linkage can be derived from:

$$\frac{d\psi_r}{dt} = -\frac{1}{T_r}\psi_r + \frac{L_m}{T_r} i_{sd} \quad (15)$$

The switching control laws of two stator current controllers are designed as follows:

$$u_{sd}^s = k_{sd}\text{sign}(s_1) \quad (16)$$

$$u_{sq}^s = k_{sq}\text{sign}(s_2) \quad (17)$$

where, k_{sd} and k_{sq} are positive constants, which effect greatly the performance of control system.

Therefore, two stator current controllers can be described as follow:

$$u_{sd} = u_{sd}^{equ} + u_{sd}^s \quad (18)$$

$$u_{sq} = u_{sq}^{equ} + u_{sq}^s \quad (19)$$

To guarantee the reachability of sliding mode control, the mathematic form of this condition can be described as:

$$\dot{s}_1 s_1 < 0 \quad (20)$$

$$\dot{s}_2 s_2 < 0 \quad (21)$$

We can be informed that if a larger k_{sd} or k_{sq} is in switching control law, the speed of reaching sliding mode surface will become faster and the control system has stronger robust property. However, amplified chattering will exist in the sliding phase. On the contrary, a smaller k_{sd} or k_{sq} will slow down the reaching speed and there is reduced chattering. The selection of k_{sd} and k_{sq} is relative to the boundary of uncertainties to keep the trajectory on sliding surface. Taking into account parameter disturbances, since the boundary of these disturbances are often unknown, to trade off the robustness, k_{sd} and k_{sq} are usually chosen to be large enough. Consequently, this conservative control law will enlarge undesired chattering and degrade the performance of overall system.

THE PROPOSED METHOD

The sliding mode controller has a serious drawback that undesired chattering often exists when system states are moving on sliding surface, due to discontinuous switching control law. In order to reduce the system chattering, many methods have been proposed (Wai, 2000; Lin and Hsu, 2004; Lin *et al*., 2007). In this study, a neural network sliding mode control method is introduced to reduce the undesired chattering phenomenon.

Neural Networks (NN) have the ability to approximate nonlinear functions. A NN can approximate any smooth function to any desired accuracy, provided that the number of hidden-layer neuron is large enough. In addition, Radial Basis Function Neural Network (RBFNN) has an advantage of faster learning ability and less chance of falling into local minimum, in comparison with standard BP neural network (Tsoi, 1989). Therefore, RBFNN is quite suitable to design of the switching control law.

The RBF neural network is a three-layer forward network. The radial basis function which maps from input layer to hidden layer is nonlinear, but the output of RBF neural network is the linear combination of the output of hidden layer. Figure 2 is a block diagram of RBF neural network, which clearly describes the conventional structure of RBF network.

The output of this neural network takes the form as follow:

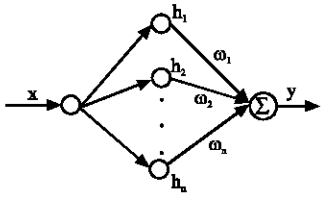

Fig. 2: Block diagram of RBF neural network

$$y = \sum_{i=1}^{n} \omega_i h_i \tag{22}$$

where, ω_i (i = 1 to n) is the weighting between hidden-layer neuron i and output-layer neuron, which is adjusted on the basis of an adaptive rule. h_i (i = 1 to n) is the output of hidden-layer neuron i.

The output of hidden-layer neurons can be defined as a Guassian function, which can be described as:

$$h_i = \exp\left[-\|x-c_i\|^2/b_i\right] \quad i = 1,2....n \tag{23}$$

where, c_i is the central position of Guassian function in hidden-layer neuron i and b_i is the spread factor of Guassian function in hidden-layer neuron i, which is a positive constant.

In this study, the RBF neural network sliding mode control is based on the combination of RBFNN and sliding mode control scheme. The conventional switching control law is replaced by the output of RBF neural network, i.e. $y = u_s$. The input of RBF neural network is the sliding function s. So the output of hidden-layer neurons can be defined as:

$$h_i = \exp\left[-\|s-c_i\|^2/b_i\right] \quad i = 1,2....n \tag{24}$$

An adaptive rule is used to adjust the weightings for optimal weighting values in the control operation. Because of the reaching condition of sliding mode control, the adaptive rule is derived from the steep descent rule to minimize the value of $\dot{s}s$. The mathematic form of adjusting weightings can be defined as:

$$E = \dot{s}s \tag{25}$$

$$\begin{aligned} d\omega_i &= -\eta\frac{\partial E}{\partial \omega_i} = -\eta\frac{\partial \dot{s}s}{\partial \omega_i} \\ &= -\eta\frac{\partial \dot{s}s}{\partial u_s}\frac{\partial u_s}{\partial \omega_i} = -\eta\frac{\partial \dot{s}s}{\partial u_s}h_i \end{aligned} \quad i = 1,2....na \tag{26}$$

where, E is the cost function and η is the adaptive rate.

In order to control the stator currents of the induction motor, two common PI current controllers are replaced by two RBF neural network sliding mode controllers. From above equations, The mathematic form of adjusting weightings in two currents controllers can be derived as:

$$\begin{aligned} d\omega_i^{sd} &= -\eta_{sd}\frac{\partial E_{sd}}{\partial \omega_i^{sd}} = -\eta_{sd}\frac{\partial \dot{s}_1 s_1}{\partial \omega_i^{sd}} \\ &= -\eta_{sd}\frac{\partial \dot{s}_1 s_1}{\partial u_{sd}^s}\frac{\partial u_{sd}^s}{\partial \omega_i^{sd}} = -\eta_{sd}\frac{\partial \dot{s}_1 s_1}{\partial u_{sd}^s}h_i^{sd} \\ &= \eta_{sd}\dot{s}_1 h_i^{sd}/\sigma L_s \end{aligned} \quad i = 1,2....nsd \tag{27}$$

$$h_i^{sd} = \exp\left[-\left\|s_1-c_i^{sd}\right\|^2/b_i^{sd}\right] \quad i = 1,2....nsd \tag{28}$$

$$u_{sd}^s = \sum_{i=1}^{nsd} \omega_i^{sd} h_i^{sd} \tag{29}$$

$$\begin{aligned} d\omega_i^{sq} &= -\eta_{sq}\frac{\partial E_{sq}}{\partial \omega_i^{sq}} = -\eta_{sq}\frac{\partial \dot{s}_2 s_2}{\partial \omega_i^{sq}} = -\eta_{sq}\frac{\partial \dot{s}_2 s_2}{\partial u_{sq}^s}\frac{\partial u_{sq}^s}{\partial \omega_i^{sq}} = -\eta_{sq}\frac{\partial \dot{s}_2 s_2}{\partial u_{sq}^s}h_i^{sq} \\ &= \eta_{sq}\dot{s}_2 h_i^{sq}/\sigma L_s \end{aligned} \quad i = 1,2....nsq \tag{30}$$

$$h_i^{sq} = \exp\left[-\left\|s_2-c_i^{sq}\right\|^2/b_i^{sq}\right] \quad i = 1,2....nsq \tag{31}$$

$$u_{sq}^s = \sum_{i=1}^{nsq} \omega_i^{sq} h_i^{sq} \tag{32}$$

where, ω_i^{sd} and ω_i^{sq} are the weighting between hidden-layer neuron i and output-layer neuron in d-axis stator and q-axis stator current controllers, respectively. η_{sd} and η_{sq} denote the adaptive rates in d-axis stator and q-axis stator current controllers, respectively. h_i^{sd} and h_i^{sq} are the output of hidden-layer neuron i in d-axis stator and q-axis stator current controllers, respectively. c_i^{sd} and b_i^{sd} are the central position and the spread factor of Guassian function in d-axis stator current controller, likewise, c_i^{sq} and b_i^{sq} are the central position and the spread factor of Guassian function in q-axis stator current controller. Therefore, the weightings between hidden-layer neurons and output-layer neurons can be adjusted online to achieve the learning ability.

SIMULATION RESULTS AND ANALYSIS

In order to validate the effectiveness of the proposed stator currents control strategy, the simulation of this strategy is performed in MATLAB/SIMULINK software.

The parameters of the induction motor used in this simulation are shown in Table 1. In addition, the overall structure of vector control technique in the induction motor can be shown in Fig. 3. In this simulation, the parameters of PI controllers are initially tuned by the Ziegler-Nichols method, then they are tuned through simulation to get satisfactory response. The parameters of RBF neural network in the proposed control scheme are as follows: the adaptive rates η_{sd} = 0.1 and η_{sq} = 0.05; the central position vectors c^{sd} = [10.5 5.25 2.62 1.31 0 -1.31 -2.62 -5.25 -10.5] and c^{sq} = [30 15 7.5 3.75 0 -3.75 -7.5 -15 -30]; the spread factor vectors b^{sd} = [0.8 0.8 0.8 0.8 0.8 0.8 0.8 0.8 0.8] and b^{sq} = [14 14 14 14 14 14 14 14 14], the initial weightings are zero.

Table 1: Parameter of induction motor

Parameter	Value
Stator resistance (Ω)	0.8130
Rotator resistance (Ω)	0.5310
Number of pole pairs	2.0000
Inertia (kg*m^2)	0.0200
Stator induction (H)	0.1063
Rotator induction (H)	0.1088
Mutual induction (H)	0.1024
Rated speed (r min^{-1})	1480.0000
Rated torque (N*M)	18.0000
Rated voltage (V)	380.0000

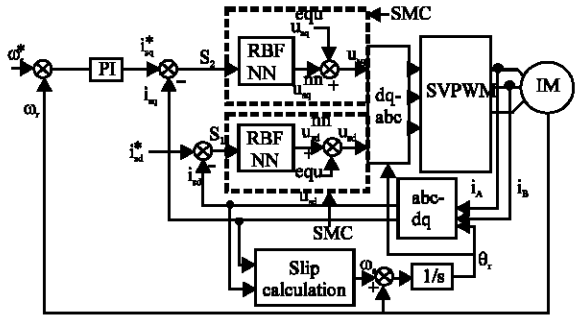

Fig. 3: Block diagram of the simulation system

Response to a step change in q-axis reference current: This simulation compares the performance of RBF sliding mode controllers and conventional PI controllers, when a step change in q-axis reference current occurs. In this comparative simulation, the induction motor starts from a standstill state, the motor speed follows a command that starts from zero and begins to accelerate at time t = 1.0s until the rotor speed is 1200 r min^{-1}, the d-axis reference current is 2A. Figure 4a-d show the response of motor using conventional PI current controllers. As may be observed, the step in i_q^* obviously disturbs the waveform of i_d at time t = 1.0 sec, when conventional PI controllers are used in current loop. Figure 5a-d show the stator current i_d is undisturbed under the same conditions, using the proposed control scheme.

Response to a step change in d-axis reference current: We compare the performance of RBF sliding mode controllers and conventional PI controller when a step change in d-axis reference current is applied. The induction motor starts from a standstill state, the d-axis reference current is 2A and has a step change (from 2A to 1A at t = 1.5 sec), the motor speed follows a command that starts from zero and begins to accelerate at time t = 1.0 sec

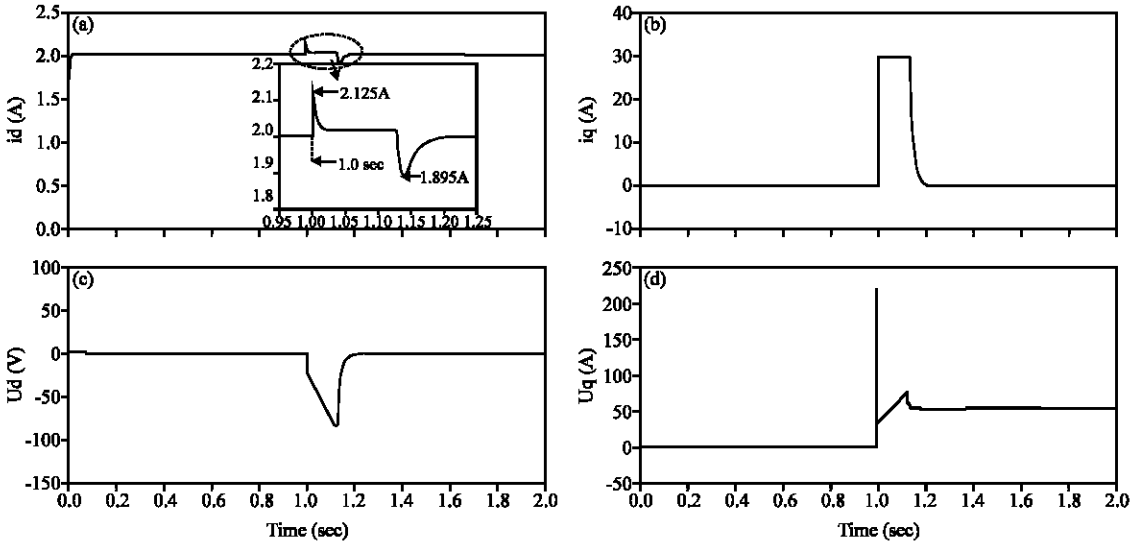

Fig. 4: Simulated response to a step change in q-axis reference current using PI controllers. (a) d-axis current response (b) q-axis current response (c) d-axis voltage response and (d) q-axis voltage response

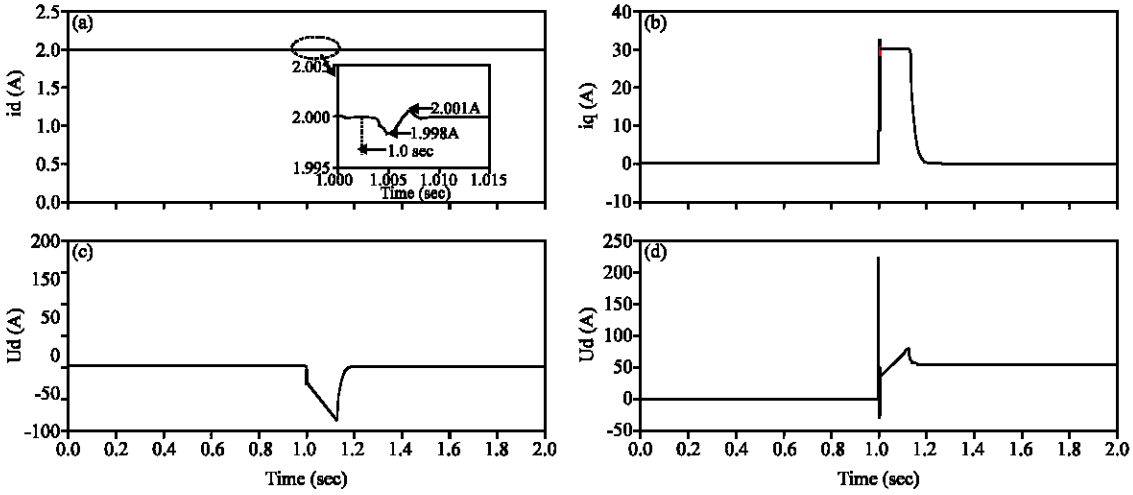

Fig. 5: Simulated response to a step change in q-axis reference current using RBF-sliding mode controllers. (a) d-axis current response (b) q-axis current response (c) d-axis voltage response and (d) q-axis voltage response

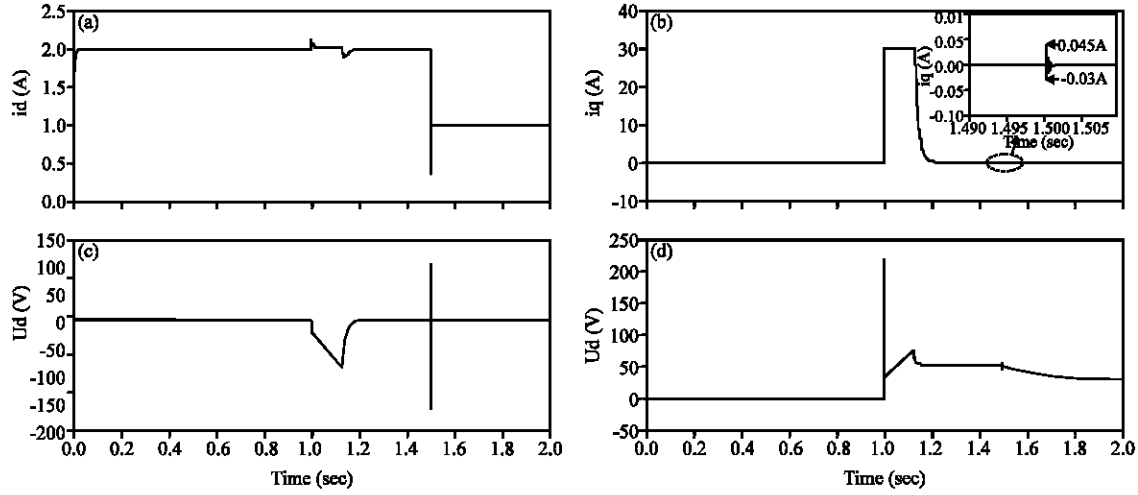

Fig. 6: Simulated response to a step change in d-axis reference current using PI controllers. (a) d-axis current response (b) q-axis current response (c) d-axis voltage response and (d) q-axis voltage response

until the rotor speed is 1200 r min^{-1}. Figure 6a-d depicts the response of motor using conventional PI current controllers. It is obvious that the step in i_d^* disturbs the waveform of i_q at time t = 1.5 sec, when conventional PI controllers are used in current loop. Figure 7a-d depict the stator current i_q is undisturbed under the same conditions, using RBF sliding mode control scheme.

Response to a step change in stator resistance: This simulation validates the effectiveness of the proposed control scheme, concerning a step change in stator resistance (from 0.813 to 1.626 Ω at 1.4 sec). The induction motor starts from a standstill state, the d-axis reference current is 2A, the motor speed follows a command that starts from zero and begins to accelerate at time t = 1.0 sec until the rotor speed is 1200 r min^{-1}. It is evident that the proposed control scheme offers a good response with little disturbance in stator current in Fig. 8 and 9.

Comparison of chattering: The objective of this simulation is the comparison of undesired chattering between RBF neural network sliding mode controllers and conventional sliding mode controllers. Conventional sliding mode controllers are used in controlling stator currents in this experiment. The parameters of conventional sliding mode controllers are as: k_{sd} = 110 and k_{sq} = 10. The induction motor starts from a standstill state, the d-axis reference current is 2A, the motor speed follows

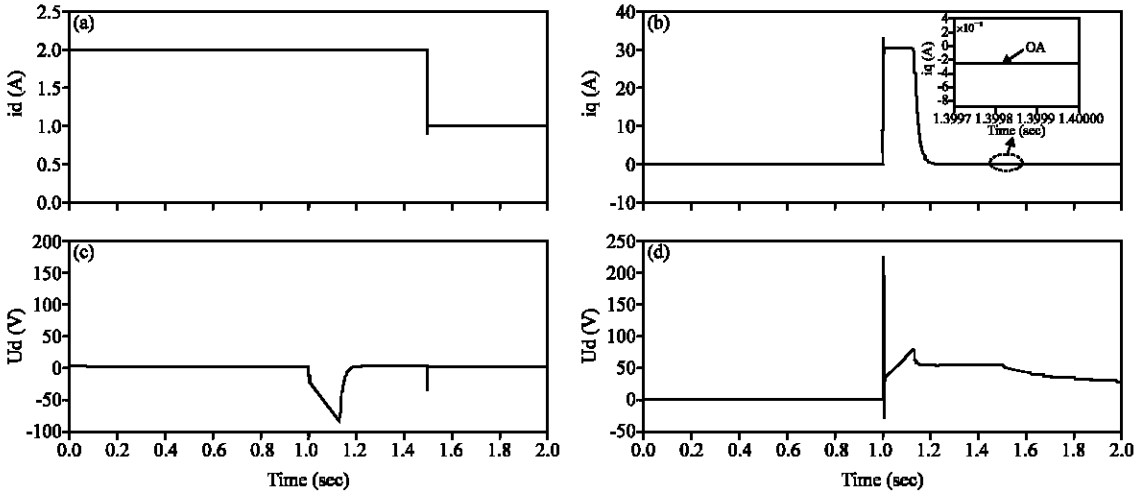

Fig. 7: Simulated response to a step change in d-axis reference current using RBF-sliding mode controllers. (a) d-axis current response (b) q-axis current response (c) d-axis voltage response and (d) q-axis voltage response

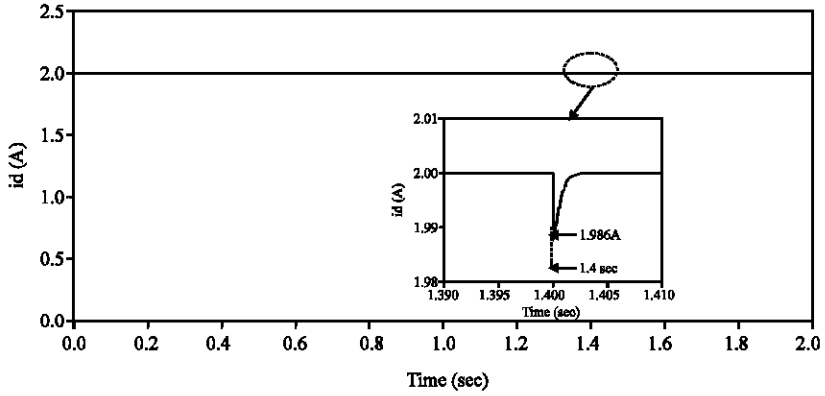

Fig. 8: Simulated response of d-axis current to a step change in stator resistance at 1.4 sec

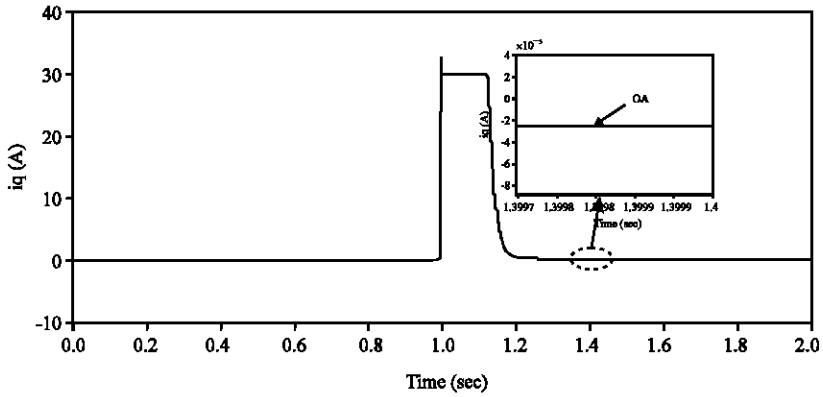

Fig. 9: Simulated response of q-axis current to a step change in stator resistance at 1.4 sec

a command that starts from zero and begins to accelerate at time t = 1.0 sec until the rotor speed is 1200 r min^{-1}. Figure 10a, b show little chattering is in RBF neural network sliding mode controllers in current loop. On the contrary, Fig. 11a and b show serious chattering obviously exists in conventional sliding mode controllers.

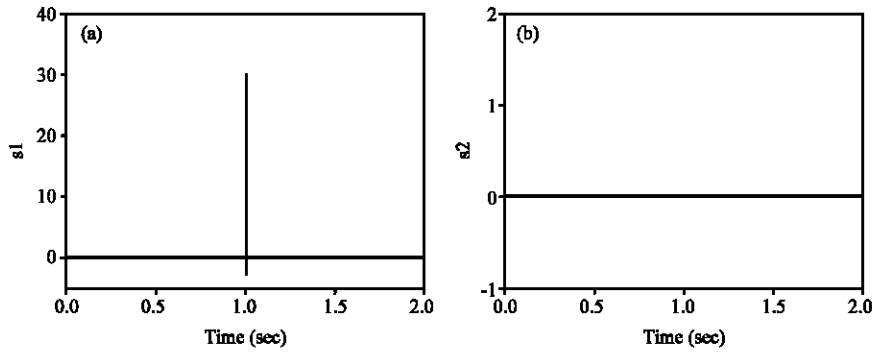

Fig. 10: Simulation results of sliding mode surface using RBF sliding mode controllers. (a) d-axis current sliding mode surface and (b) q-axis current sliding mode surface

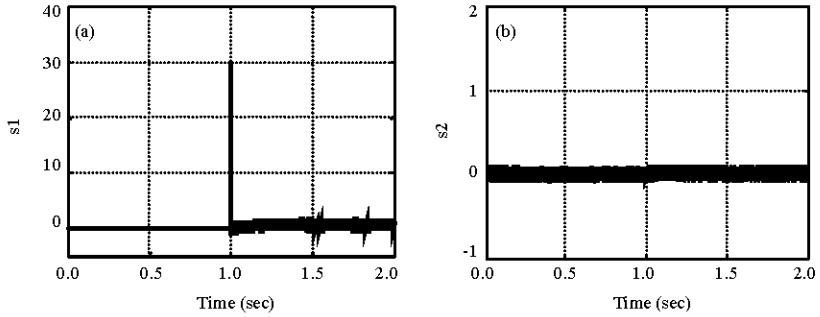

Fig. 11: Simulation results of sliding mode surface using conventional sliding mode controllers. (a) d-axis current sliding mode surface and (b) q-axis current sliding mode surface

It shows clearly that RBF neural network sliding mode design can reduce undesired chattering considerably.

CONCLUSIONS

This study has investigated the coupling problem of stator currents in induction motor. A new method has been presented in this study to achieve the current decoupling, which is based on the combination of sliding mode control and RBF neural network. As with the conventional SMC, the proposed scheme can reduce chattering notably. The simulation results have validated the satisfactory performance of the proposed method, such as perfect decoupling, strong robustness and reduced chattering, in comparison with PI and conventional SMC.

ACKNOWLEDGMENT

Thanks for the support of the National Natural Science Foundation of China (No.60874047) Peng Kang and Zhao Jin developed the concept. Peng Kang performed the simulation using MATLAB software from April, 2009 to March, 2010 in Institute of Automation, Huazhong University of Science and Technology, Wuhan, China

REFERENCES

Bose, B.K., 2002. Modern Power Electronics and AC Drives. 2nd Edn., Prentice Hall, Upper Saddle River, New Jersey, USA., ISBN-10: 013016743, pp: 736.

Harnefors, L. and H.P. Nee, 1998. Model-based current control of AC machines using the internal model control method. IEEE Trans. Ind. Appl., 34: 133-141.

Holtz, J., J. Quan, J. Pontt, J. Rodriguez, P. Newman and H. Miranda, 2002. Design of fast and robust current regulators for high-power drives based on complex state variables. IEEE Trans. Ind. Applied, 17: 772-778.

Jung, J., S. Lim and K. Nam, 1997. PI type decoupling control scheme for high speed operation of induction motors. Proceedings of Power Electronics Specialists Conference (PESC), June 22-27, St Louis, MO, USA, pp: 1082-1085.

Jung, J., S. Lim and K. Nam, 1997. PI type decoupling control scheme for high speed operation of induction motors. Proceedings of Power Electronics Specialists Conference (PESC), June 22-27, St Louis, MO, USA, pp: 1082-1085.

Lasaad, S., Z. Dalila and A.M. Naceurq, 2007. Adaptative variable structure control for an online tuning direct vector controlled induction motor drives. J. Applied Sci., 7: 3177-3186.

Lin, C.M. and C.F. Hsu, 2004. Adaptive fuzzy sliding-mode control for induction servomotor systems. IEEE Trans. Energy Conversion, 19: 362-368.

Lin, F.J., L.T. Teng and P.H. Shieh, 2007. Intelligent sliding-mode control using RBFN for magnetic levitation system. IEEE Trans. Ind. Electr., 54: 110-116.

Ma, Z., T. Zheng, F. Lin and X.J. You, 2005. A new sliding-mode controller for field oriented controlled induction motor drives. Proceedings of 31th Annual Conference of the IEEE Industrial Electronics Society, Nov. 6, Raleigh, NC, pp: 1341-1346.

Tsoi, A.C., 1989. Multilayer percepton trained using radial basis functions. Elecr. Lett., 25: 1296-1297.

Utkin, V.I., 1993. Sliding mode control design principles and applications to electric drives. IEEE Trans. Ind. Electr., 40: 23-36.

Wai, R.J., 2000. Adaptive sliding-mode control for induction servomotor drives. IEE Pwc. Cleclr. Power Appl., 147: 553-562.

Young, K.D., V.I. Utkin and U. Ozguner, 1999. A control engineer's guide to sliding mode control. IEEE Trans., 7: 328-341.